Polymer 49 (2008) 5186–5190

Contents lists available at ScienceDirect

Polymer

journal homepage: www.elsevier.com/locate/polymer

Polymer Communication

Real-time investigation of crystallization in poly(vinylidene fluoride)-based nano-composites probed by infrared spectroscopy

Kumiko Asai [a], Masami Okamoto [a,*], Kohji Tashiro [b]

[a] Advanced Polymeric Nanostructured Materials Engineering, Graduate School of Engineering, Toyota Technological Institute, 2-12-1 Hisakata, Tempaku, Nagoya 468 8511, Japan
[b] Department of Future Industry-oriented Basic Science and Materials, Graduate School of Engineering, Toyota Technological Institute, 2-12-1 Hisakata, Tempaku, Nagoya 468 8511, Japan

ARTICLE INFO

Article history:
Received 25 July 2008
Received in revised form 9 September 2008
Accepted 27 September 2008
Available online 9 October 2008

Keywords:
Poly(vinylidene fluoride)
Nano-composites
Crystallization

ABSTRACT

Via time-resolved Fourier transform infrared spectroscopy (FTIR), we examined the real-time investigation of the conformational changes of poly(vinylidene fluoride) (PVDF) chain segment during crystallization of neat PVDF and the corresponding nano-composites having intercalated structure. It was shown that in the following crystallization processes the crystal growth was virtually the same in both nano-composites and neat PVDF. We have examined an annealing at an infinitely long time at 200 °C (~20 min) to erase the thermal history in the nano-composites. The dispersed titanate nano-filler particles exhibited strong contribution to enhance the heterogeneous nucleation for the formation of both γ- and β-phase crystals.

© 2008 Elsevier Ltd. All rights reserved.

1. Introduction

A new polymorph of poly(vinylidene fluoride) (PVDF) was introduced in PVDF-based nano-composites [1–4]. The phase is preferentially crystallized in the β polymorph in the presence of the organically modified montmorillonite (organo-clay). They reported that similar crystal lattices between clay and the β polymorph, and the large flat surface of the clay are the key factors to interact between polymer and inorganic materials [4].

In our previous paper [5], we described the effect of the nano-filler particles on the crystallization kinetics and crystalline structure of poly(vinylidene fluoride) (PVDF) upon nano-composite formation. We specifically discussed the crystallization behavior and its kinetics including the conformational changes of the PVDF chain segment during crystallization of neat PVDF and nano-composite by using differential scanning calorimetry, wide angle X-ray diffraction, light scattering (LS), and infrared spectroscopic analyses.

The neat PVDF predominantly formed α-phase in the crystallization temperature range of 110–150 °C. On the other hand, PVDF/layer titanate (HTO) nano-composite exhibiting mainly α-phase crystal coexists with γ- and β-phase at low T_c range (110–135 °C). The major γ-phase crystal appeared at high T_c (=140–150 °C), owing to the dispersed layer titanate particles as a nucleating agent. The overall crystallization rate and crystalline structure of pure PVDF were strongly influenced in the presence of layered titanate particles [5].

Unfortunately, as discussed in previous paper, we could not employ LS photometry due to the big negative birefringence originated from the dispersed silicate (montmorillonite (MMT) and synthetic fluorine hectorite (*syn*-FH) [6]) nano-fillers in matrix PVDF as compared with that of well-crystallized neat PVDF. So far, the studies on the crystallization kinetics in PVDF/*syn*-FH system have been restricted by LS experiment.

Recently, a full analysis of the crystallization of PVDF in nano-composites has been done by Dillon et al. [7] and Buckley et al. [8]. Using Fourier transform infrared spectroscopy (FTIR), they reported that α-form coexists with β- and γ-phase, and the amount of β-phase increases with increasing MMT-clay content. However, we know, by now, that the crystallization kinetics of the nano-composites is not very well explored in the literatures except our previous paper [5]. In this regard, we need to pin down the crystallization kinetics of the PVDF/silicate nano-composites.

To better understand the kinetics, time-resolved Fourier transform infrared spectroscopy (FTIR) is a very powerful tool on the basis of the skeletal and chain conformational changes of the PVDF during isothermal crystallization. It motivated us to investigate the time development of the different polymorph in the PVDF upon nano-composite formation.

In this communication, *via* FTIR, we examined the real-time investigation of the conformational changes of the PVDF chain segment

* Corresponding author. Fax: +81 (0)52 809 1864.
E-mail address: okamoto@toyota-ti.ac.jp (M. Okamoto).

0032-3861/$ – see front matter © 2008 Elsevier Ltd. All rights reserved.
doi:10.1016/j.polymer.2008.09.061

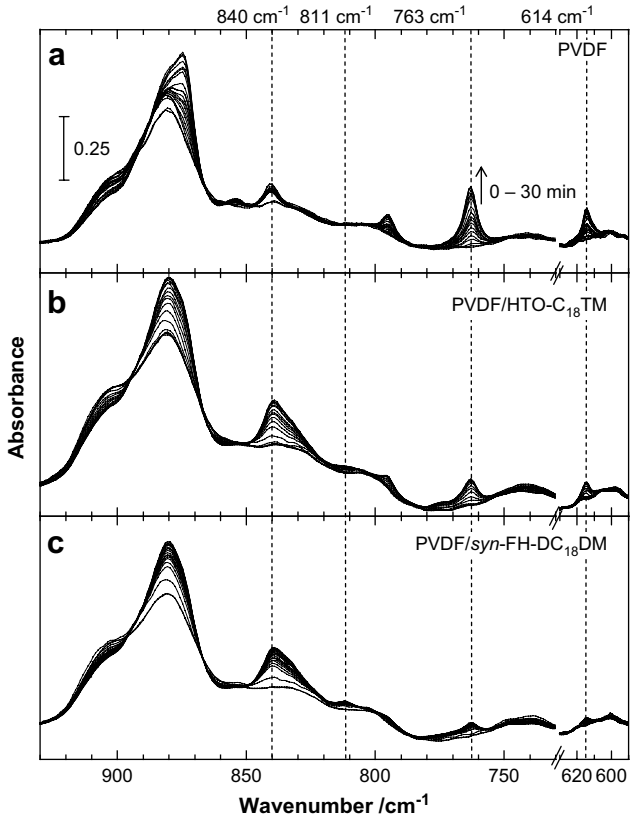

Fig. 1. Time-resolved spectra of (a) neat PVDF, (b) PVDF/HTO-C_{18}TM and (c) PVDF/*syn*-FH-DC_{18}DM in the region of 930–590 cm^{-1} during isothermal crystallization for 30 min at 130 °C after annealing at 200 °C for 3 min.

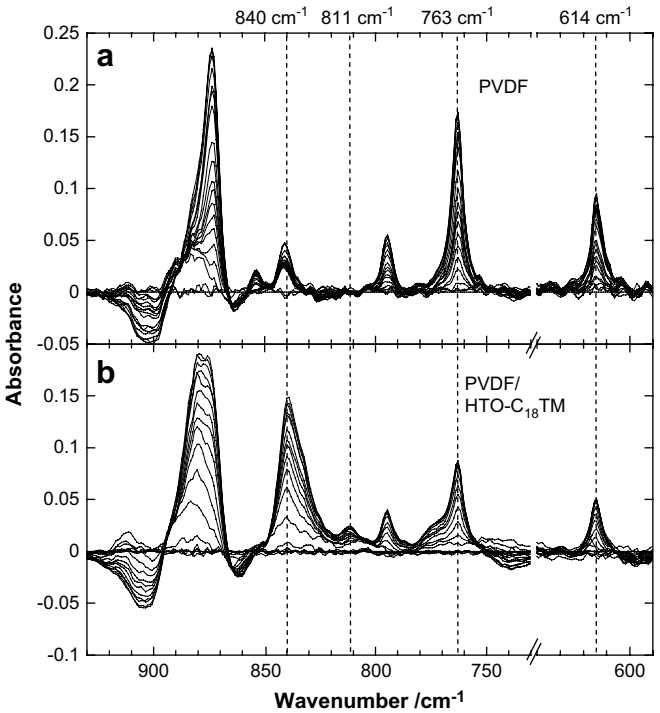

Fig. 2. Difference spectra of (a) neat PVDF and (b) PVDF/HTO-C_{18}TM in the region of 930–590 cm^{-1}.

during crystallization of neat PVDF and the corresponding nano-composites.

2. Experimental

2.1. Materials

The PVDF-based nano-composite used in this study was the same material used in our previous studies [5]. The nano-composite was prepared through the melt extrusion method with organically modified layered fillers (OMLFs) (HTO intercalated with octadecyl tri-methylammonium (C_{18}TM), and *syn*-FH intercalated with di-octadecyl di-methylammonium (DC_{18}DM) cations [9–11]) content of 5 wt% and henceforth will be termed as PVDF/HTO-C_{18}TM and PVDF/*syn*-FH-DC_{18}DM, using a Mini-MAX Molder (CS-183, Custom Scientific Instruments Inc.) operated at 190 °C for 4 min to yield intercalated PVDF-based nano-composite strands.

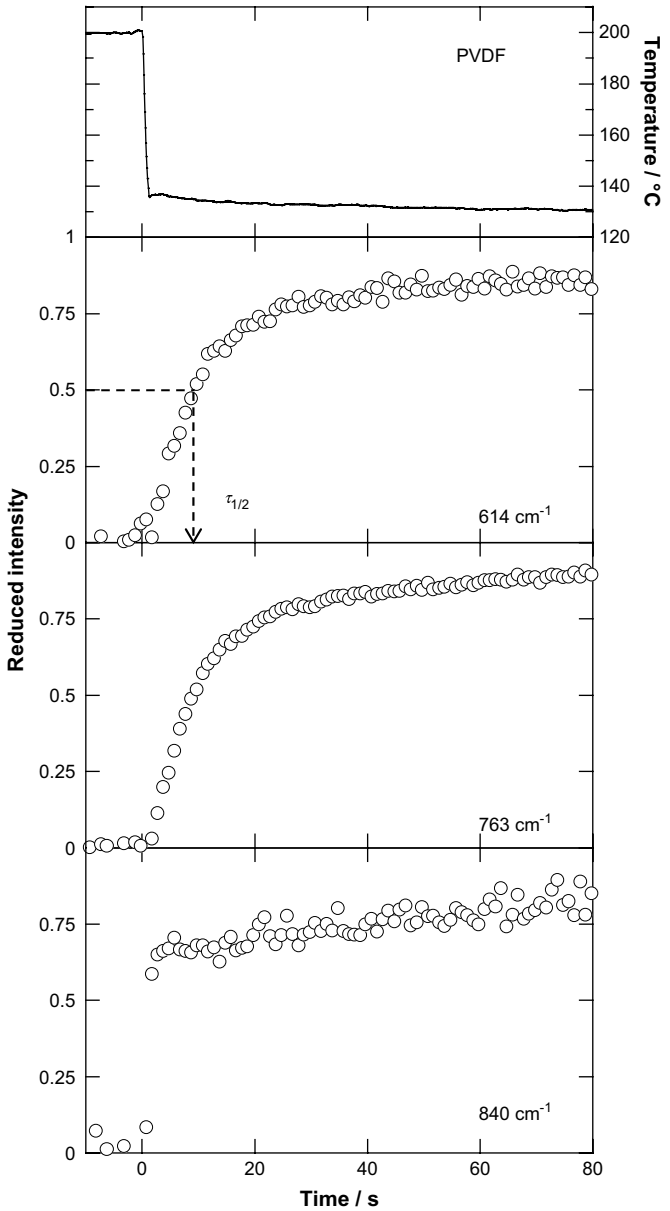

Fig. 3. Time variation of the reduced intensities for the characteristic bands in neat PVDF taken at 130 °C. The arrow indicates the crystallization *half-time* $\tau_{1/2}$. Upper panel indicates temperature drop profile during crystallization of the sample.

The PVDF-based nano-composites exhibited well-ordered intercalated structure. Details regarding the structure analysis can be found in our previous paper [5].

The surface charge density is particularly important because it determines the interlayer structure of intercalants as well as cation exchange capacity (CEC). The characterizing method consists of total elemental analysis and the dimension of the unit cell [9]:

$$\text{Surface charge}: \mathrm{e^-/nm^2} = \zeta/ab \quad (1)$$

where ζ is the layer charge (1.07 for HTO and 0.66 for *syn*-FH; a and b are cell parameters of HTO ($a = 3.782$ Å, $b = 2.978$ Å [9]) and *syn*-FH ($a = 5.24$ Å, $b = 9.08$ Å [9]). For *syn*-FH, however, about 30% of the interlayer Na^+ ions are not replaced quantitatively by intercalants due to the non-active Na^+ for ion-exchange reactions [9]. For HTO, only 27% of interlayer H^+ (H_3O^+) is active for ion-exchange reactions. The remaining part is the non-active sites in the HTO. Thus the incomplete replacement of the interlayer ions is ascribed to the intrinsic chemical reactivity. HTO has highly surface charge density of 1.26 e^-/nm^2 compared with that of *syn*-FH (0.971 e^-/nm^2).

2.2. Fourier transform infrared spectroscopy (FTIR)

FTIR spectra were collected at 2 cm^{-1} nominal resolution using a Varian FTS7000 spectrometer equipped with a MCT detector in transmission mode. The spectra were obtained by averaging 32 scans with a mean collection length of 1 s per spectrum. The background spectra used for reduction were collected at the same crystallization temperature (T_c) with the sample. The homogenous

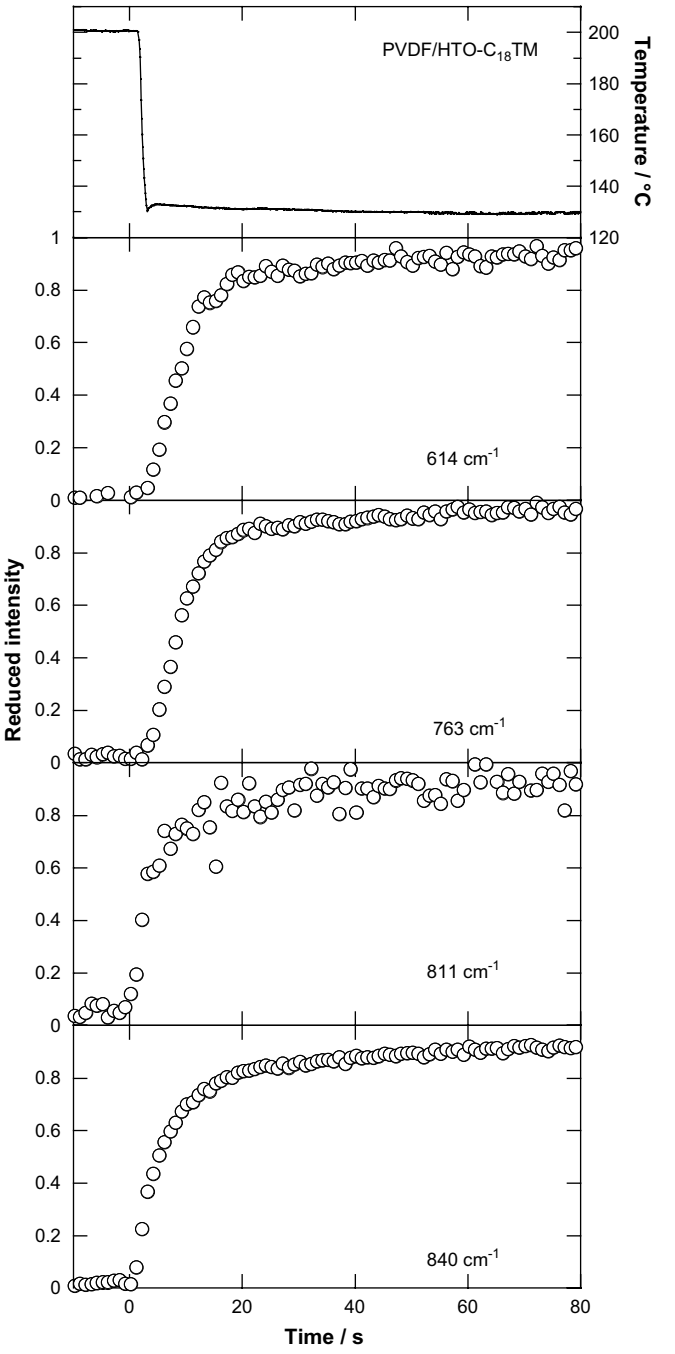

Fig. 4. Time variation of the reduced intensities for the characteristic bands in PVDF/HTO-C_{18}TM taken at 130 °C. Upper panel indicates temperature drop profile during crystallization of the sample.

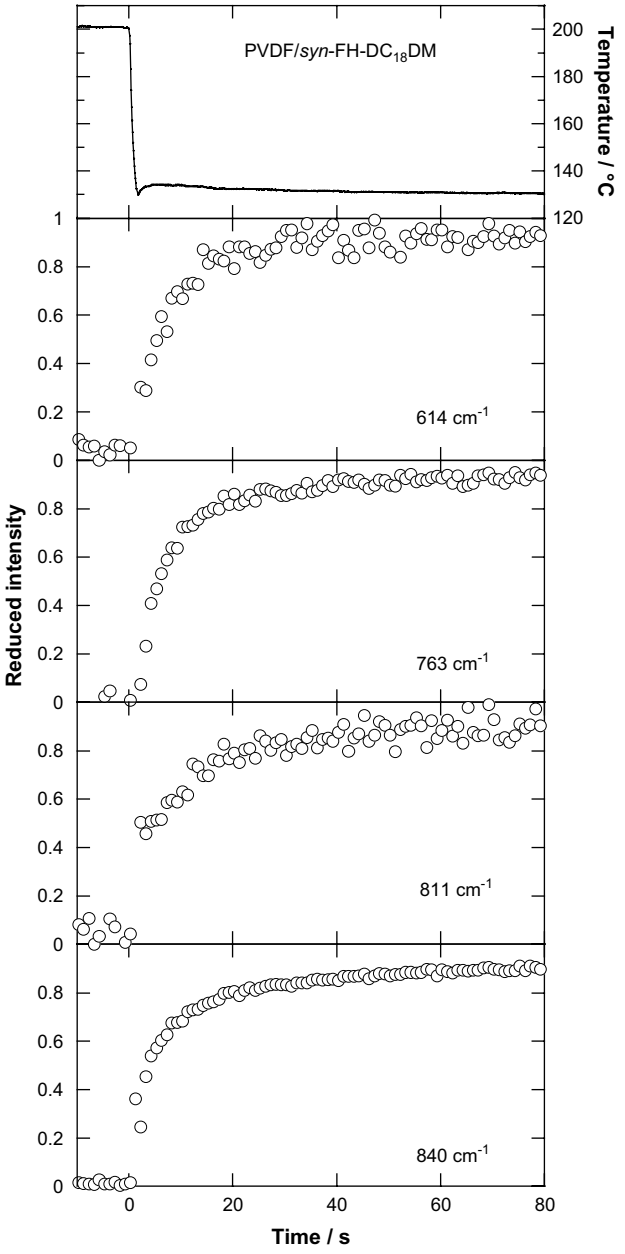

Fig. 5. Time variation of the reduced intensities for the characteristic bands in PVDF/*syn*-FH-DC_{18}DM taken at 130 °C. Upper panel indicates temperature drop profile during crystallization of the sample.

mixture of KBr powder and PVDF (fine powder) or PVDF-based nano-composites (powder) in the weight ratio 95:5 was prepared. The mixtures were then converted into disks with a thickness of ~0.4 mm by pressing. The disks were placed in a homemade environmental heating chamber, which allowed to reach the desired T_c in a very short time (~2 s). Each sample was kept at 200 °C for 3 min to erase any thermal history, and it was immediately cooled to T_c. After attaining T_c, a time-resolved FTIR measurement was carried out in the temperature range of 110–150 °C. The collected data were processed by soft ware (Grams/AI®, Thermo Galactic Co., USA).

3. Results and discussion

3.1. Time-dependent spectral evolution

Fig. 1 shows typical time-dependent spectral variations of neat PVDF and the corresponding nano-composites (PVDF/HTO-C_{18}TM and PVDF/*syn*-FH-DC_{18}DM) in the region of 930–590 cm^{-1} during isothermal crystallization at 130 °C. The frequencies and the vibrational assignments for the neat PVDF and nano-composites are reported in our previous paper [5,12]. For neat PVDF, bands located at 763 and 614 cm^{-1}, which are common to α-phase crystallite, arise and their intensities increase until the crystallization is complete (~30 min).

On the other hand, the behavior of the nano-composites for the same bands suggests the following: the small increment especially in PVDF/*syn*-FH-DC_{18}DM implies that the formation of α-phase is suppressed as compared with well-crystallized neat PVDF, while the intensity of band at 840 cm^{-1} yields a strong growth, which is an indication of long trans sequences, as characteristic of β-phase.

The time variation of the band of 811 cm^{-1} (attributed to the CH_2 rocking mode in γ-phase) for neat PVDF is negligible at 130 °C so that nothing happens up until 30 min.

By subtracting the initial spectrum of melt state (at 200 °C) from the consecutive spectra, a difference spectrum can be achieved. Fig. 2 shows the representative difference spectra of neat PVDF and PVDF/HTO-C_{18}TM corresponding to Fig. 1. The bands in the positive regions are crystalline-dependent peaks while those in the negative regions are amorphous-dependent. These results suggest that major γ-phase crystal that coexists with β- and small α-phase is formed in the nano-composite systems, while neat PVDF predominantly forms α-phase despite of the small evolution of the *TT* sequence in the molecular conformation, as discussed in our previous paper [5].

Figs 3–5 show typical examples of the time variation of the reduced intensities for the characteristic bands taken at 130 °C for neat PVDF and nano-composites. We notice that the intensity growth at 840 cm^{-1} is very rapid in neat PVDF as compared with that of the nano-composites. This feature is also observed in the temperature dependence of the crystallization rate (see Fig. 6). Then taking the crystallization *half-time* $\tau_{1/2}$ at which the reduced intensity reaches 1/2, we define $1/\tau_{1/2}$ as a measure of the overall crystallization rate at each characteristic band [13]. Now, assuming

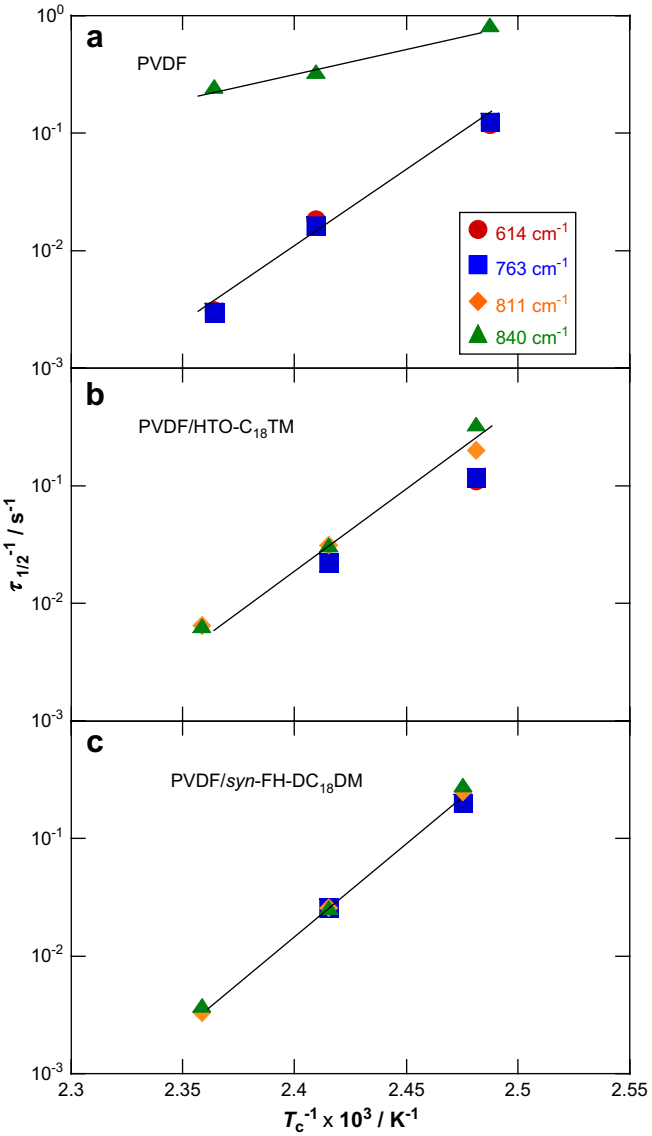

Fig. 6. Temperature dependence of the reciprocal *half-time* of the different polymorph in neat PVDF and PVDF upon nano-composite formation.

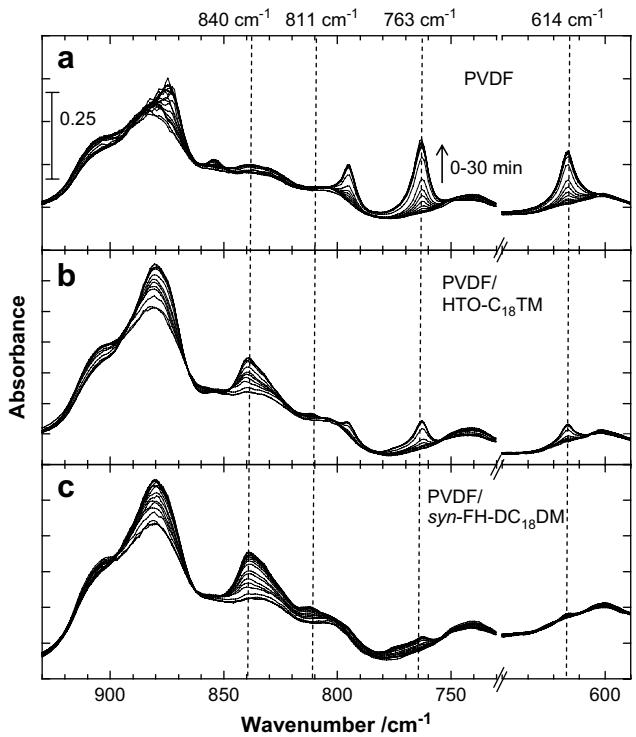

Fig. 7. Time-resolved spectra of (a) neat PVDF, (b) PVDF/HTO-C_{18}TM and (c) PVDF/*syn*-FH-DC_{18}DM in the region of 930–590 cm^{-1} during isothermal crystallization for 30 min at 130 °C after annealing at 200 °C for 20 min.

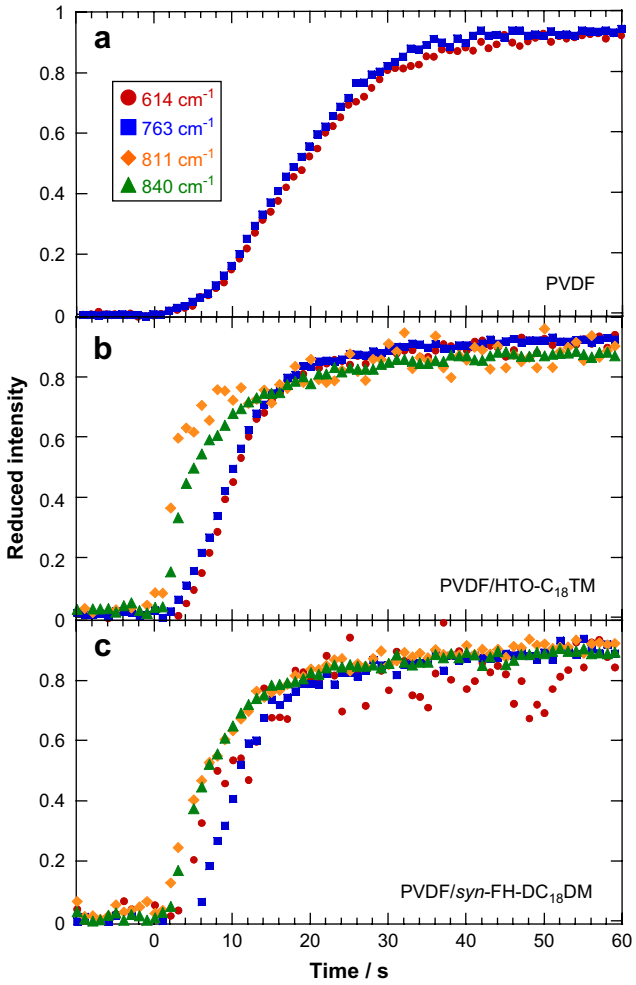

Fig. 8. Time variation of intensities of (a) PVDF, (b) PVDF/HTO-C_{18}TM and (c) PVDF/*syn*-FH-DC_{18}DM taken at 130 °C.

that the rate constant $1/\tau_{1/2}$ is of Arrhenius-type, then, $1/\tau_{1/2}$ is given as

$$1/\tau_{1/2} \sim \exp(E_a/RT) \quad (2)$$

where E_a is the activation energy for the crystallization, RT is the thermal energy.

To confirm our consideration for the crystallization kinetics, in Fig. 6 we constructed an Arrhenius plot of $1/\tau_{1/2}$ *versus* reciprocal of the absolute temperature, $1/T$, for the growth behavior of the different polymorph in the PVDF upon nano-composite formation. For neat PVDF and all nano-composite systems examined the plots nicely conform to straight lines in each characteristic band regardless of the presence of the nano-fillers. For neat PVDF, the front factor for $1/\tau_{1/2}$ *versus* $1/T$ plots for the band at 840 cm^{-1} is about ten times larger than that for the intensity growth of other bands at T_c range of 130–150 °C, as discussed above.

The slope that reflects the activation energy of the crystallization process is virtually same (~4 kJ/mol) in all nano-composite systems regardless the type of the nano-fillers having different charge density and different crystal lattice parameters. This value is comparable to the value reported for various polymer crystallization near T_m [14]. The result implies that in the following crystallization processes the chain folding mechanisms of the crystal growth are virtually the same in both nano-composites and neat PVDF (see Fig. 6(a)).

3.2. Effect of thermal history on following crystallization process

Now we turn our attention to the primary nucleation. To erase the thermal history of the systems, we examined annealing at an infinitely long time where the effect of the thermal history had been observed (it was in fact ~20 min for the samples).

Fig. 7 shows the representative time variation of the intensities of neat PVDF and the corresponding nano-composites in the region of 930–590 cm^{-1} during isothermal crystallization at 130 °C. In neat PVDF, the band at 840 cm^{-1} arose when the annealing time is 3 min, however for 20 min that band does not appear. Due to the erase of the thermal history incompletely, long trans sequences might be contained in neat PVDF. Fig. 8 shows the representative time variation of the intensities of neat PVDF and its nano-composites. In nano-composites, the intensity growth of bands is faster than that of neat PVDF. Furthermore, the bands at of 811 and 840 cm^{-1} derived from γ-phase and long trans sequences exhibit more rapid growth compared with that of 614 and 763 cm^{-1}. That is, the dispersed nano-filler particles have strong contribution to enhance the heterogeneous nucleation as seen in Fig. 7 (induction time t_0 *versus* crystallization temperature T_c plot) in our previous paper [5].

Further studies are currently in progress to elucidate the effect of thermal history on the crystallization in the nano-composites and will be clarified shortly [15].

4. Conclusions

Via time-resolved FTIR, we have investigated the conformational changes of the PVDF chain segment during crystallization of neat PVDF and the corresponding nano-composites having intercalated structure (PVDF/HTO-C_{18}TM and PVDF/*syn*-FH-DC_{18}DM). It was shown that in the following crystallization processes the crystal formation was virtually the same in both nano-composites and neat PVDF. The activation energy of the crystallization process is virtually same (~4 kJ/mol) in all nano-composite systems regardless the type of the nano-fillers having different charge density and different crystal lattice parameters [5]. We have examined an annealing at an infinitely long time at 200 °C (~20 min) to erase the thermal history in the PVDF/HTO-C_{18}TM system. The dispersed titanate nano-filler particles exhibited strong contribution to enhance the heterogeneous nucleation for the formation of both γ- and β-phase crystals.

Acknowledgements

This work was supported by the MEXT "Collaboration with Local Communities" Project (2005–2009).

References

[1] Priya L, Jog JP. J Polym Sci Part B Polym Phys 2002;40:1682.
[2] Priya L, Jog JP. J Polym Sci Part B Polym Phys 2003;41:31.
[3] Priya L, Jog JP. J Appl Polym Sci 2003;89:2036.
[4] Giannelis EP, Shah D, Maiti P, Gunn E, Schmidt DF, Jiang DD. Adv Mater 2004; 16:1173.
[5] Asai K, Okamoto M, Tashiro K. Polymer 2008;49:4298.
[6] Greene KR. Clay Miner 1970;8:405.
[7] Dillon DR, Tenneti KK, Li CY, Ko FK, Sics I, Hsiao BS. Polymer 2006;47:1678.
[8] Buckley J, Cebe P, Cherdack D, Crawford J, Ince BS, Jenkins M, et al. Polymer 2006;47:2411.
[9] Yoshida O, Okamoto M. Macromol Rapid Commun 2006;27:751.
[10] Saito T, Okamoto M, Hiroi R, Yamamoto M, Shiroi T. Polymer 2007;48:4143.
[11] Sinha Ray S, Yamada K, Okamoto M, Ogami A, Ueda K. Chem Mater 2003; 15:1456.
[12] Kobayashi M, Tashiro K, Tadokoro H. Macromolecules 1975;8:158.
[13] Kubo H, Okamoto M, Kotaka T. Polymer 1998;39:4827.
[14] Hoffman JD. Polymer 1983;24:3.
[15] Asai K, Okamoto M, Tashiro K, in preparation.